

# Offsets between H $\alpha$ and CO arms of a spiral galaxy NGC 4254: A New Method for Determining the Pattern Speed of Spiral Galaxies

Fumi EGUSA, Yoshiaki SOFUE, and Hiroyuki NAKANISHI

*Institute of Astronomy, University of Tokyo*

*fegusa@ioa.s.u-tokyo.ac.jp, sofue@ioa.s.u-tokyo.ac.jp, hnakanis@ioa.s.u-tokyo.ac.jp*

(Received 2004 September 8; accepted 2004 October 9)

## Abstract

We examined offsets between HII regions and molecular clouds belonging to spiral arms of a late type spiral galaxy NGC 4254 (M99). We used a high resolution  $^{12}\text{CO}$  ( $J=1-0$ ) image obtained by Nobeyama Millimeter Array (NMA) and an H $\alpha$  image. We derived angular offsets ( $\theta$ ) in the galactic disk, and found that these offsets show a linear dependence on the angular rotation velocity of gas ( $\Omega_G$ ). This linear relation can be expressed by an equation:  $\theta = (\Omega_G - \Omega_P) \cdot t_{\text{H}\alpha}$ , where  $\Omega_P$  and  $t_{\text{H}\alpha}$  are constant. Here,  $\Omega_P$  corresponds to the pattern speed of spiral arms and  $t_{\text{H}\alpha}$  is interpreted as the timescale between the peak compression of the molecular gas in spiral arms and the peak of massive star formation. We may thus determine  $\Omega_P$  and  $t_{\text{H}\alpha}$  simultaneously by fitting a line to our  $\theta - \Omega_G$  plot, if we assumed they are constant. From our plot, we obtained  $t_{\text{H}\alpha} = (4.8 \pm 1.2) \times 10^6$  yr and  $\Omega_P = 26_{-6}^{+10}$  km s $^{-1}$  kpc $^{-1}$ , which are consistent with previous studies. We suggest that this  $\theta - \Omega_G$  plot can be a new tool to determine the pattern speed and the typical timescale needed for star formations.

**Key words:** galaxies: fundamental parameters—galaxies: individual(NGC 4254, M99)—galaxies: spiral—ISM: molecules—ISM: HII region

## 1. Introduction

### 1.1. Pattern Speed

Pattern speed ( $\Omega_P$ ) is defined as an angular rotation velocity of spiral pattern. According to the spiral density wave theory (Lin & Shu 1964),  $\Omega_P$  determines the location and even the existence of resonances, which would greatly affect the morphology and kinematics of a galaxy. The results of numerical simulations also show the large dependence of spiral structure on  $\Omega_P$  (Sempere et al. 1995). Despite its importance on the study of galaxies, it cannot be determined directly from observations, since the pattern structure is not a material but a density wave propagating through the disk.

Several methods have been proposed to date for the determination of pattern speed. Tremaine & Weinberg (1984) presented the method using the continuity equation for the surface brightness of galaxies. Canzian (1993) showed that the residual velocity field, obtained by subtracting the axisymmetric component from observed velocity field, has a difference in pattern between the inside and outside of the corotation. Cepa & Beckman (1990) pointed out that where the arm to interarm ratio of star formation efficiency has a sharp dip could be thought as the corotation. These methods work well for some galaxies, but there are still inconsistencies or large uncertainties.

### 1.2. CO and H $\alpha$

In this letter, we examined offsets between H $\alpha$  and CO arms of a spiral galaxy. We suggest that we can use them as a new method for the determination of pattern speed

and typical timescale for star formation.

The H $\alpha$  emission is the tracer of HII region, which surrounds newly born massive stars, while the CO emission is the tracer of molecular gas. According to the galactic shock wave theory (Fujimoto 1968; Roberts 1969), most molecular clouds are formed and then condensed by the compression owing to the spiral shock wave and thus belong to the spiral arm. Since galactic scale star formations take place in these molecular arms, some molecular gases are used to form stars, and the others are dissociated by UV emission from massive stars born in that star formation. In consequence, molecular clouds disappear soon after their formation and their position appears to be fixed to the spiral pattern, though individual molecular clouds move at the speed of gas. Therefore, the position of spiral pattern and H $\alpha$  arm can be measured by using that of a molecular arm and an ensemble of HII regions respectively. In other words, offset between the arms of H $\alpha$  and CO represents the difference between the speed of gas and spiral pattern, as well as the time needed for star formation from molecular clouds.

This offset has been found in many spiral galaxies (eg. Rand & Kulkarni 1990). We can easily see it in a  $B$ -band image as a displacement of an arm's peak and a dust lane, since the light of  $B$ -band is mainly emitted by the young OB star and the distribution of dust lane and molecular gas are almost the same. However, this offset has not been studied quantitatively yet, since the resolution of the CO image was too large to examine detail structures of spiral arms.

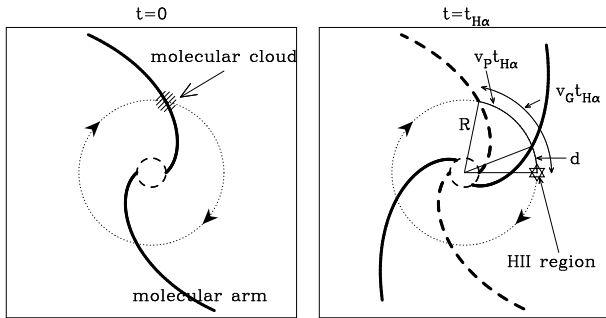


**Fig. 1.** The basic idea of our method. If we observe a face-on spiral galaxy at  $t=0$  (the left panel), the same galaxy will be observed as the right panel at  $t=t_{\text{H}\alpha}$ . The thick solid lines are molecular arms at the time  $t$  of each panel. The thick dashed lines in the right panel ( $t=t_{\text{H}\alpha}$ ) show the position of molecular arms in the left panel ( $t=0$ ). The offset distance between H $\alpha$  and CO arm is  $d$ , expressed in equation (1).

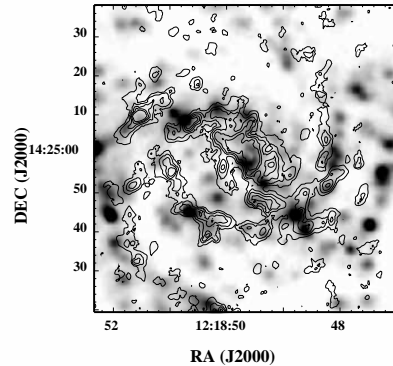


**Fig. 2.** Projected image of NGC 4254: CO contours on an H $\alpha$  image.

## 2. A Method for Determining the Pattern Speed

We assume that the pattern of spiral is rigid, and that the gas rotates in circular orbit. Then we define a timescale  $t_{\text{H}\alpha}$  as an *average* time for H $\alpha$  arm to develop from a galactic-shock-compressed molecular arm. If the physical processes of star formation are not extremely different in the spiral disk, this timescale can be regarded as a constant parameter representing a typical value of the entire disk.

Figure 1 illustrates this idea for the inside of the CR. If we observe a face-on spiral galaxy at  $t=0$  (the left panel), at  $t=t_{\text{H}\alpha}$  the same galaxy will be observed as the right panel and the offset distance between the arms of H $\alpha$  and CO,  $d$ , can be written as

$$d = \left( \frac{v_G}{\text{km s}^{-1}} \right) \left( \frac{t_{\text{H}\alpha}}{\text{s}} \right) - \left( \frac{v_P}{\text{km s}^{-1}} \right) \left( \frac{t_{\text{H}\alpha}}{\text{s}} \right) \quad [\text{km}], \quad (1)$$

where  $v_G$  is the velocity of gas, and  $v_P$  is the velocity of pattern. We adopt this expression, in which  $d$  becomes a positive value, since most of molecules exist in a rather central part of the disk and thus they seem to be in the inside of the CR. If molecular gas is more extended and the outside of the CR should be taken into account, H $\alpha$  arm will be seen on the concave side of CO arm and  $d$  will be negative.

Dividing both sides of equation (1) by radius  $R$  [kpc], we obtain

$$\theta = \left\{ \left( \frac{\Omega_G}{\text{km s}^{-1} \text{ kpc}^{-1}} \right) - \left( \frac{\Omega_P}{\text{km s}^{-1} \text{ kpc}^{-1}} \right) \right\} \times \left( \frac{t_{\text{H}\alpha}}{\text{s}} \right) \quad [\text{km kpc}^{-1}], \quad (2)$$

where  $\Omega_G \equiv v_G/R$ ,  $\Omega_P \equiv v_P/R$ , and  $\theta$  is the azimuthal offset. This equation shows the relation between two observables,  $\Omega_G$  and  $\theta$ , and we can rewrite it as

$$\theta \simeq 0.58(\Omega_G - \Omega_P) t_{\text{H}\alpha} \quad (3)$$

where  $\theta$  is in degree and  $t_{\text{H}\alpha}$  is in  $10^7$  yr. If we assume that  $t_{\text{H}\alpha}$  is constant in a certain range of radius in a galaxy,  $\theta$  becomes a linear function of  $\Omega_G$ , since we assume the

rigid pattern, in other words, constant  $\Omega_P$ . Therefore, by plotting  $\theta$  against  $\Omega_G$  and fitting them with a line, both  $\Omega_P$  and  $t_{\text{H}\alpha}$  can be determined at the same time. In addition, the linearity of this plot can verify the validity of the assumptions we made. We discuss this validity in section 4.

## 3. Data

We observed a SAc galaxy NGC 4254 in the  $^{12}\text{CO}$  ( $J=1-0$ ) line using Nobeyama Millimeter Array during a long-term project, ‘‘Virgo high resolution CO survey’’ (Sofue et al. 2003a). The spatial resolution is about 2 arcsec, which corresponds to  $\sim 160$  pc at a distance from the Virgo cluster of 16.1 Mpc. This resolution is small enough to trace the spiral arms with typical width of 1 kpc. For more detailed information about this galaxy and the CO observation, see Sofue et al. (2003c).

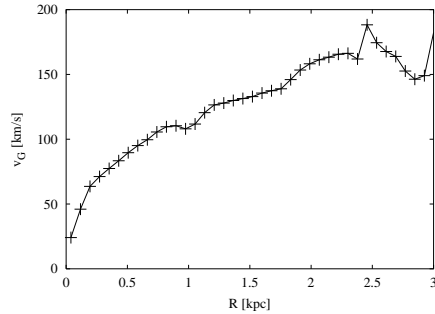
Koopmann et al. (2001) presented broadband  $R$  and narrowband H $\alpha$  images of 63 spiral galaxies in the Virgo cluster. The resolution of the image is 1.2 arcsec, comparable to that of our CO data. We determined the coordinate of the H $\alpha$  image using the Galactic stars seen in the  $R$  band image, since these two images had the same field of view. The typical uncertainty of this coordinate fitting is about 1 arcsec, smaller than the resolution of the images. We show an overlaid image of CO and H $\alpha$  in Figure 2.

As we see in this figure, it is nearly face-on (We derived an inclination angle as  $34^\circ$  for central region. See the following paragraph for detail.) and has well-ordered spiral arms (classified as arm class 9 by Elmegreen & Elmegreen (1987)), so that the spiral structure can be easily traced. This is why we selected this galaxy to examine offsets between H $\alpha$  and CO arms.

Position angle (P.A.) and inclination ( $i$ ) are also important parameters of a galaxy. We determined them applying the task ‘GAL’ of AIPS to the velocity field of CO. This task cuts annuli out from a velocity field, and fits

**Table 1.** Position angle and inclination of NGC 4254

	P.A. [°]	$i$ [°]
Schweizer (1976)	58	29
Iye et al. (1982)	70	42
Phookun et al. (1993)	68	42
This letter (2003)	72	34

**Fig. 3.** Rotation curve of NGC 4254, determined by CO velocity field.

them with a pure circular rotation velocity field in order to derive P.A. and  $i$  at each radius. We averaged the derived values at  $5'' < r < 16''$ , corresponding to  $0.4 \text{ kpc} < r < 1.2 \text{ kpc}$ , where the values do not change largely, and then obtained P.A. =  $72^\circ \pm 4^\circ$  and  $i = 34^\circ \pm 5^\circ$ . In Table 1, these P.A. and  $i$  are listed with values from other papers. Although only the central region was used in this work, the determined values are not so different from previous work, in most of which the whole image of the galaxy was used for the determination.

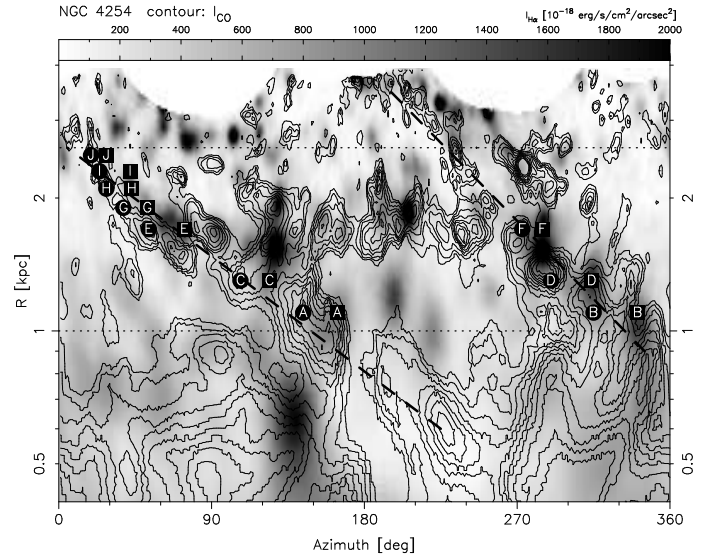
Using the obtained P.A. and  $i$ , we calculated the rotation velocity of gas by the use of 'GAL' again. The resultant rotation curve (Figure 3) is not perfectly the same with that derived by the iteration method (Takamiya & Sofue 2002; Sofue et al. 2003b), since they used the different value of P.A. and  $i$ .

These P.A. and  $i$  were also used to deproject the image into a face-on view and to transform it into a polar-coordinate image, a phase diagram (Figure 4). Azimuth is taken to be zero at the NW side of minor axis and to increase clockwise, in the same direction of this galaxy's rotation assuming the trailing arms. A range between the two horizontal lines in this figure ( $1 \text{ kpc} < r < 2.6 \text{ kpc}$ ) show the region used in the following analysis. Filled boxes and circles are the peaks of H $\alpha$  and CO intensity, respectively. See the following section for detail.

## 4. Application and Result

### 4.1. Deriving Offsets

We divided the phase diagram into strips of 200 pc radial width, averaged the intensity with respect to radius at each azimuth in each strip, and plotted the averaged intensity against azimuth. We defined an offset angle  $\theta$  as an azimuthal angular separation of intensity peaks be-

**Fig. 4.** Phase diagram of NGC 4254: CO contours on H $\alpha$  image. Thick dashed lines indicate rough positions of two marked spiral arms. Filled circles and boxes are the peaks of CO arm and H $\alpha$  arm, respectively, which are defined by the analysis described in section 4. Labels, from A to J, are to identify these peaks and offsets presented in Figure 5. The region between the two horizontal lines ( $1 \text{ kpc} < r < 2.6 \text{ kpc}$ ) indicates where we used in the analysis.

tween the H $\alpha$  and CO arms. Since arms of this galaxy are not totally continuous and have some breaks, we could not find corresponding peaks at some radii. In addition, we only used the range of  $1 \text{ kpc} < r < 2.6 \text{ kpc}$ , since the spiral feature is not clear in the inner region and the rotation curve has a large dispersion in the outer region (See Figure 3). In Figure 4, this range is indicated by two horizontal lines. The peak of CO and H $\alpha$  arm is marked by a filled and labeled circle and box, respectively, with a label from A to J, corresponding to that in Figure 5.

The largest factor for the error in  $\theta$  is the resolution of CO data, which is about 2 arcsec. Thus this error is written as

$$\Delta\theta \simeq 8.9 \times \left(\frac{R}{\text{kpc}}\right)^{-1} \quad [\text{deg}]. \quad (4)$$

In addition, the uncertainty of the coordinate fitting of H $\alpha$  image and the fact that the determination of offset angles is somewhat subjective would also be possible sources of error in  $\theta$ . We, however, neglected these errors for the simplicity of calculations, so that the error in  $\theta$  could be larger than the value obtained from equation (4) by a factor of 2 at most.

### 4.2. Fitting

We plotted the derived offsets against  $\Omega_G$ , derived from rotation curve (Figure 5). Errorbars in offset angle are  $\Delta\theta$ , calculated from equation (4) at each radius. We used the  $\chi$ -square fitting method and obtained  $t_{\text{H}\alpha} = (4.8 \pm 1.2) \times 10^6 \text{ yr}$  and  $\Omega_P = 26_{-6}^{+10} \text{ km s}^{-1} \text{ kpc}^{-1}$ . The dashed line in Figure 5 is the fitted line, and the gradient and

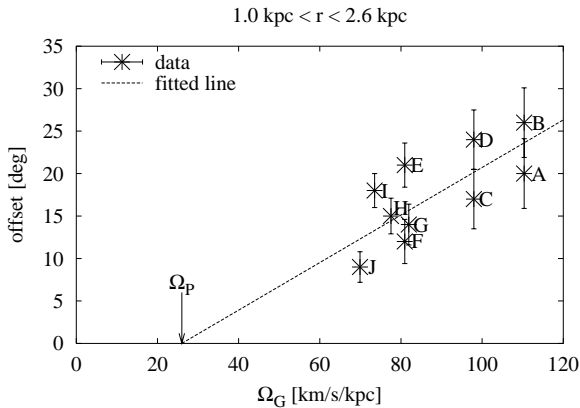


**Fig. 5.** The plot of offset angles against the angular rotation velocity. Labels, from A to J, are to identify the offsets, corresponding to the intensity peaks in Figure 4. Errorbars are calculated from equation (4) and the dashed line is the fitted line obtained by the  $\chi$ -square method. The horizontal-axis-intercept and the gradient of this line corresponds to  $\Omega_P$  and  $t_{H\alpha}$ , respectively.

horizontal-axis-intercept of this line corresponds to the resultant value of  $t_{H\alpha}$  and  $\Omega_P$ , respectively.

Kranz et al. (2001) showed that the corotation radius for the same galaxy is about 7.5 kpc from numerical simulations, and corresponding  $\Omega_P$  is about  $20 \text{ km s}^{-1} \text{ kpc}^{-1}$ . They assumed the distance to the galaxy as 20 Mpc. If we adjust this result to the distance of 16.1 Mpc,  $\Omega_P$  should be about  $25 \text{ km s}^{-1} \text{ kpc}^{-1}$ . The typical timescale of star formation has been suggested as about  $10^7$  yr from the calculation of Jeans time in molecular clouds. Our results are in good agreement with these previous studies.

#### 4.3. Discussion

In our method, we assumed a pure circular rotation and a constant time delay for star formation from molecular clouds, and we did not do any correction for extinction in  $H\alpha$  data. We however know that deviations from these assumptions are not critically large. The streaming motion and the velocity dispersion would generate some non-circular motion, but in a spiral disk, these are usually about  $10 \text{ km s}^{-1}$  (Adler & Westpfahl 1996; Combes & Becquaert 1997), which is very small compared to the circular rotation velocity of  $\sim 100 \text{ km s}^{-1}$ . The validity of the latter assumption, constant  $t_{H\alpha}$ , can be checked by the linearity of  $\theta - \Omega_G$  plot (Figure 5). Since this plot is well fitted with a line, dependence of  $t_{H\alpha}$  on the environment should be small and included in the error of the derived value.

The extinction of  $H\alpha$  is surely significant to luminosity and this might lead us to overestimate the offset values, since the amount of extinction becomes larger as HII regions get closer to molecular arms and an  $H\alpha$  arm thus seems to shift to the downstream side from where it really is. González & Graham (1996) showed azimuthal brightness profiles of NGC 4254 in  $K_s$ -,  $g$ -, and  $r_s$ -band image at  $R=75''$  (Figure 20 in their paper). Though the shape

of profile is different from one to another, the positions of peak brightness are well consistent among them. Hence, we can assume that the extinction would hardly change the position of  $H\alpha$  arms and neglect the effect of extinction on the offset values.

## 5. Conclusion

We examined the offset between the arm of  $H\alpha$  and CO of SAc galaxy NGC 4254, derived ten offset values and found the linear relation between the offset angle and the angular rotation velocity. This linearity implies that a rigid spiral pattern exists and that the physical processes of star formation can be regarded as not to extremely change in the disk. We emphasize that this is the first work to show this relationship.

With this relation, we derived the pattern speed  $\Omega_P = 26_{-6}^{+10} \text{ km s}^{-1} \text{ kpc}^{-1}$ , and the time delay for star formation  $t_{H\alpha} = (4.8 \pm 1.2) \times 10^6$  yr. We again emphasize that we can derive both  $\Omega_P$  and  $t_{H\alpha}$  simultaneously. Since the obtained values are consistent with previous studies, the way of our analysis can be a new method for the determination of the pattern speed and the typical timescale needed for star formations. Thus, this method can investigate not only the kinematics, but also the star formation mechanisms quantitatively. Moreover, this method can be applied to many spiral galaxies, since offsets between  $H\alpha$  and CO arms have been found in many spirals.

We are very grateful to Rebecca A. Koopmann, Jeffrey D. P. Kenney, and Judith Young for kindly providing us with their  $R$  and  $H\alpha$  image of NGC 4254. H. N. is financially supported by a Research Fellowship from the Japan Society for the Promotion of Science for Young Scientists.

## References

- Adler, D. S., & Westpfahl, D. J. 1996, AJ, 111, 735
- Canzian, B. 1993, ApJ, 414, 487
- Cepa, J. & Beckman, J. E. 1990, ApJ, 349, 497
- Combes, F., & Becquaert, J-F. 1997, A&A, 326, 554
- de Vaucouleurs, G., de Vaucouleurs, A., Corwin, H. G. Jr., Buta, R. J., Paturel, G., & Fouqué P. 1991, Third Reference Catalog of Bright Galaxies (New York: Springer-Verlag)
- Elmegreen, D. M., & Elmegreen, B. G. 1987, ApJ, 314, 3
- Ferrarese, L., Freedman, W. L., Hill, R. J., Saha, A., Madore, B. F., Kennicutt, R. C. Jr., Stetson, P. B., Ford, H. C., et al. 1996, ApJ, 464, 568
- Fujimoto, M. 1968, IAUS, 29, 453
- González, R. A., & Graham, J. R. 1996, ApJ, 460, 651
- Gerssen, J., Kuijken, K., & Merrifield, M. R. 1999, MNRAS, 306, 926
- Iye, M., Okamura, S., Hamabe, M., & Watanabe, M. 1982, ApJ, 256, 103
- Koopmann, R. A., Kenney, J. D., & Young, J. 2001, ApJS, 135, 125
- Kranz, T., Slyz, A., & Rix, H-W. 2001, ApJ, 562, 164
- Lin, C. C. & Shu, F. H. 1964, ApJ, 140, 646
- Phookun, B., Vogel, S. N., & Mundy, L. G. 1993, ApJ, 418, 113
- Rand, R. J. & Kulkarni, S. R. 1990, ApJ, 349, L43

- Roberts, W. W. 1969, ApJ, 158, 123  
Sempere, M. J., García-Burillo, S., Combes, F., & Knapen, J. H. 1995, *ã*, 296, 45  
Schweizer, F. 1976, ApJS, 31, 313  
Sofue, Y., Koda, J., Nakanishi, H., Onodera, S., Kohno, K., Tomita, A., & Okumura, S. K. 2003, PASJ, 55,17  
Sofue, Y., Koda, J., Nakanishi, H., & Onodera, S. 2003, PASJ, 55, 59  
Sofue, Y., Koda, J., Nakanishi, H., & Hidaka, M. 2003, PASJ, 55, 75  
Takamiya, T., & Sofue, Y. 2002, ApJL, 576, L15  
Tremaine, S. & Weinberg, M. D. 1984, ApJ, 282, L5  
Tully, R. B. 1974, ApJS, 27, 449